STABILITY ANALYSIS FOR BUOYANCY-OPPOSED FLOWS IN POLOIDAL DUCTS OF THE DCLL BLANKET

N. Vetcha, S. Smolentsev and M. Abdou

Fusion Science and Technology Center at University of California, Los Angeles, CA, 90095, vnaveen@fusion.ucla.edu

An approach developed in earlier work to study the hydrodynamic stability of the buoyancy assisted flow in DCLL blanket based on the solution of the Orr-Sommefeld equation for MHD flows is used here to address the stability of the buoyancy-opposed (downward) flows in the DCLL blanket conditions. The present analysis predicts that downward flows in DCLL blanket conditions will likely be hydrodynamically unstable and eventually turbulent due to the development of either inflectional instability or boundary layer instability.

I. INTRODUCTION

In the dual-cooled lead-lithium (DCLL) blanket, which is considered in the US for testing in ITER and for using in DEMO, the eutectic alloy lead-lithium (PbLi) circulates slowly (at ~ 10 cm/s) for power conversion and tritium production (Fig. 1). In this blanket, the most of heat deposition and tritium breeding occur in the poloidal ducts facing the plasma (front ducts) where the forced flow is superimposed with buoyant flows, resulting in the mixed convection flow regime. The preliminary analysis of mixed convection under the ITER and DEMO blanket conditions[1] has shown that buoyant flows in the long poloidal ducts are comparable with or can even dominate over forced flows, thus affecting heat transfer and tritium transport. The goal of the present study is to identify conditions when buoyancy opposed flows in the poloidal ducts become unstable, as significant changes in heat and tritium transport are likely to occur if the flow in the blanket transients to being unstable.

In our earlier work,[2] the hydrodynamic stability of the buoyancy-assisted (upward) flows is studied analytically using a linear stability theory based on the modified Orr-Sommerfeld equation that takes into account specific DCLL blanket conditions. It was concluded that in these conditions buoyancy assisted flows are linearly stable. Under fusion blanket conditions these liquid metal flows are known to become quasi- two-dimensional[3] (Q2D) due to a kind of magnetic diffusion associated with a strong toroidal magnetic field. This striking feature allows using Q2D flow equations, known

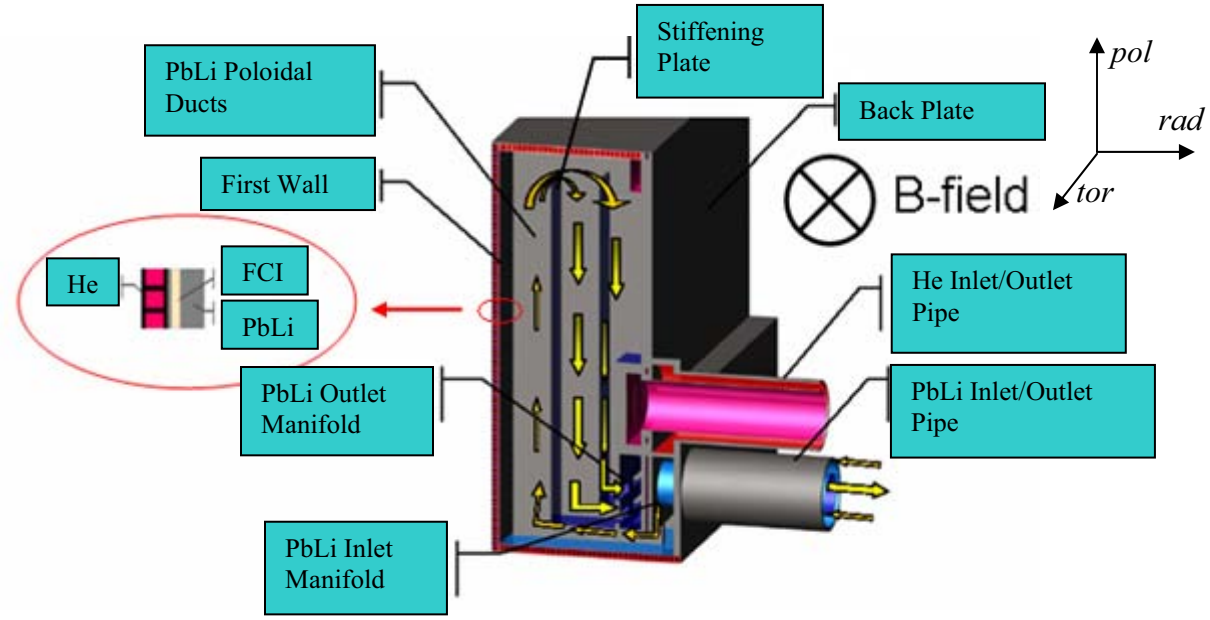

Fig. 1. Sketch of the US DCLL DEMO blanket module (Ref. 1).

as SM82 equations.[3] An analytical solution for the downward flow case basic flow is derived[4] based on these SM82 equations. Modified Orr-Sommerfeld equation is derived by imposing small perturbations on the basic solution, and then the obtained eigen value problem is solved numerically using a pseudo-spectral method.

The obtained numerical data are plotted in the form of neutral curves, which can be used to predict transitions from a steady mixed flow to the unsteady one, where heat and mass transport are strongly controlled by large coherent vortical structures.

II. PROBLEM FORMULATION

The flow investigated in this paper is mixed convection flow of liquid metal PbLi in the presence of a transverse (toroidal) magnetic field B_0, which is driven by an external pressure gradient and also affected by a buoyancy force associated with the volumetric heating $\dot{q}$ due to neutrons. The volumetric heating changes rapidly in the radial direction (y) and is approximated here with the following formula:

$$\dot{q} = q_0 e^{-(y+a)/l},$$

where the ratio $a/l \equiv m$ is hereafter referred to as the "shape parameter".

The present analysis is limited to those ducts of the DCLL blanket, where the forced flow is downwards. A schematic of this system is shown in Fig. 2 and typical dimensionless parameters are summarized in Table I for both the DEMO (Ref. 1) and ITER (Ref. 1) blanket.

TABLE I. Basic Dimensionless Flow Parameters in the Poloidal Flow in the Front Duct for ITER and DEMO (for definition of *Ha*, *Re* and *Gr*, see Section III)

Parameter	ITER	DEMO
Ha	6500	12,000
Re	30,000	60,000
Gr	7.0×10^{9}	2.0×10^{12}
m	0.3	1.0

Such flows, generally unsteady, are governed by a system of Q2D equations, written in the Boussinesq approximation, in terms of the velocity components $U(t,x,y)$ and $V(t,x,y)$, the pressure $P(t,x,y)$, and the temperature $T(t,x,y)$:[1]

$$\frac{\partial U}{\partial t}+U\frac{\partial U}{\partial x}+V\frac{\partial U}{\partial y}=-\frac{1}{\rho}\frac{\partial P}{\partial x}+\nu\left(\frac{\partial^2 U}{\partial x^2}+\frac{\partial^2 U}{\partial y^2}\right)-\frac{U}{\tau} \qquad (1)$$
$$+g+g\beta(T_0-T),$$

$$\frac{\partial V}{\partial t}+U\frac{\partial V}{\partial x}+V\frac{\partial V}{\partial y}=-\frac{1}{\rho}\frac{\partial P}{\partial y}+\nu\left(\frac{\partial^2 V}{\partial x^2}+\frac{\partial^2 V}{\partial y^2}\right)-\frac{V}{\tau}, \qquad (2)$$

$$\rho C_p\left(\frac{\partial T}{\partial t}+U\frac{\partial T}{\partial x}+V\frac{\partial T}{\partial y}\right)=\kappa\left(\frac{\partial^2 T}{\partial x^2}+\frac{\partial^2 T}{\partial y^2}\right)+\dot{q}, \qquad (3)$$

$$\frac{\partial U}{\partial x}+\frac{\partial V}{\partial y}=0. \qquad (4)$$

Here, $\rho,\nu,\sigma,\kappa,C_p,\beta$ are the fluid density, kinematic viscosity, electrical conductivity, thermal conductivity, specific heat and volumetric thermal expansion coefficient respectively. g is the acceleration due to gravity, L is the duct length, $2a\times 2b$ are the duct cross-sectional dimensions, τ is the Hartmann braking time[3], and T_0 is the mean bulk temperature at the flow inlet. In the present analysis, we assume ideal electrical and thermal insulation. In the real blanket conditions, near-perfect insulation can be achieved using the so-called flow channel insert made of Silicon carbide composite or foam.[4] In the conditions of near-perfect electrical insulation, $\tau = b(\rho/\sigma\nu)^{1/2}$. In what follows, a modified form of the energy equation is used by introducing a new function $\theta(t,x,y)$, such that:

$$T(t,x,y) = T_0 + \frac{\bar{q}}{\rho C_p U_0}x + \theta(t,x,y) \qquad (5)$$

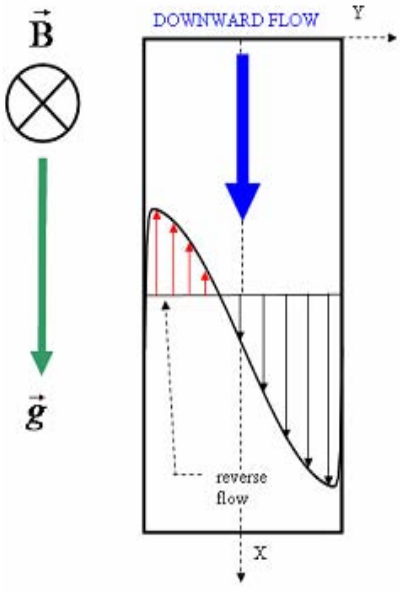

Fig. 2. Sketch illustrating the forced flow direction with respect to the gravity vector and magnetic field.

where U_0 stands for the mean bulk velocity, and $\bar{q} = (2a)^{-1}\int_{-a}^{a}\dot{q}(y)dy$ is the mean volumetric heating.

III. LINEAR STABILITY ANALYSIS

In the linear stability analysis, infinitesimal disturbances are imposed on steady laminar basic flow. The basic flow has only one velocity component: $\bar{U}(y)$. By introducing the above said disturbances, the velocity, pressure and temperature fields can be written as

$$U = \bar{U} + u', V = v', P = \bar{P} + p', \theta = \bar{\theta} + \theta', \quad (6)$$

where the prime denotes an infinitesimal disturbance which is a function of x, y and t. The basic flow is a solution of Eqs. (1-4). However, the resulting motion in Eq. (6) also has to satisfy these equations. Inserting Eq. (6) in the governing equations and ignoring all small terms quadratic in perturbations, we obtain

$$\frac{\partial u'}{\partial t} + \bar{U}\frac{\partial u'}{\partial x} + \frac{\partial \bar{U}}{\partial y}v' = -\frac{\partial p'}{\partial x} + \frac{1}{Re}\left(\frac{\partial^2 u'}{\partial x^2} + \frac{\partial^2 u'}{\partial y^2}\right) - \frac{Gr}{Re^2}\theta' - \frac{Ha}{Re}\left(\frac{a}{b}\right)^2 u', \quad (7)$$

$$\frac{\partial v'}{\partial t} + \bar{U}\frac{\partial v'}{\partial x} = -\frac{\partial p'}{\partial y} + \frac{1}{Re}\left(\frac{\partial^2 v'}{\partial x^2} + \frac{\partial^2 v'}{\partial y^2}\right) - \frac{Ha}{Re}\left(\frac{a}{b}\right)^2 v', \quad (8)$$

$$\frac{\partial \theta'}{\partial t} + \bar{U}\frac{\partial \theta'}{\partial x} + \frac{\partial \bar{\theta}}{\partial y}v' = \frac{1}{RePr}\left(\frac{\partial^2 \theta'}{\partial x^2} + \frac{\partial^2 \theta'}{\partial y^2} - u'\right), \quad (9)$$

$$\frac{\partial u'}{\partial x} + \frac{\partial v'}{\partial y} = 0. \quad (10)$$

Here, $Re = U_0 a/\nu$, $Gr = g\beta\bar{q}a^5/\kappa\nu^2$, $Ha = B_0 b\sqrt{\sigma/\rho\nu}$ and $Pr = \rho C_p \nu/\kappa$ are the Reynolds, Grashof , Hartmann and the Prandtl number respectively.

By expanding the solution in normal modes, the disturbances can be represented by

$$\psi'(x, y, t) = \varphi(y)e^{i(\alpha x - \beta t)}, \quad (11)$$

$$\theta'(x, y, t) = h(y)e^{i(\alpha x - \beta t)}, \quad (12)$$

where $\psi'(x,y,t)$ is the stream function for the two-dimensional perturbation ($u' = \partial\psi'/\partial y, v' = -\partial\psi'/\partial x$). Here α is real, so that $\lambda = 2\pi/\alpha$ is the wavelength of the perturbation. The quantity β is complex: $\beta = \beta_r + i\beta_i$. The ratio β_r/α is the propagation velocity of the flow perturbation, also known as the "phase velocity". The parameter β_i (amplification factor) determines whether a perturbation is amplified or damped with time: the flow is stable, neutrally stable or unstable for $\beta_i < 0$, $\beta_i = 0$ or $\beta_i > 0$, respectively. The amplitude functions $\varphi(y)$ and $h(y)$ are set to be only dependent on y, since the basic flow is only dependent on y. Equation (11) yields the components of the perturbation velocity as

$$u' = \frac{\partial \varphi}{\partial y}e^{i(\alpha x - \beta t)}, \quad (13)$$

$$v' = -i\varphi(y)e^{i(\alpha x - \beta t)}. \quad (14)$$

Inserting Eqs. (12), (13) and (14) in Eqs. (7), (8) and (9), and eliminating the pressure, the following coupled ordinary differential equations are found for the amplitude functions $\varphi(y)$ and $h(y)$:

$$i\alpha\,\mathrm{Re}((\bar{U} - \beta/\alpha)(\varphi'' - \alpha^2\varphi) - \bar{U}''\varphi) = \varphi^{iv} - 2\alpha^2\varphi'' + \alpha^4\varphi - \frac{Gr}{\mathrm{Re}}h' - Ha\left(\frac{a}{b}\right)^2(\varphi'' - \alpha^2\varphi), \quad (15)$$

$$i\alpha\,\mathrm{Re}\,\mathrm{Pr}((\bar{U} - \beta/\alpha)h - \bar{\theta}'\varphi) = h'' - \alpha^2 h - \varphi', \quad (16)$$

where prime denotes differentiation with y. Equations (15) and (16) show that instability can appear either due to inflection points in the basic velocity profile (Eq. 15) or due to temperature variations (Eq. 16). The latter, however, introduces weaker instability mechanism compared to the Kelvin-Helmholtz (inflectional) instability associated with the inflection points.[5] This simplifies the problem by eliminating the need for solving Eq. (16).

IV. NUMERICAL METHOD

The stability analysis is now reduced to an eigenvalue problem for the perturbation differential equation, Eq. (15) without the term with h', with the following boundary conditions; which provide no-slip at the walls.

$$y = -1 : u' = v' = 0 : \varphi = 0, \varphi' = 0, \quad (17a)$$

$$y = +1 : u' = v' = 0 : \varphi = 0, \varphi' = 0. \quad (17b)$$

For a given basic flow $\overline{U}(y)$, Eq. (15) contains six parameters, namely $Re, Gr, Ha, \alpha, \beta_i$ and β_r. Of these parameters, Reynolds, Grashof and Hartmann numbers of the basic flow can be considered as given, and in addition the wavelength $\lambda = 2\pi/\alpha$ of the perturbation can also be taken as given. Therefore, for every set of these parameters, the differential equation with the specified boundary conditions yields an eigenfunction $\varphi(y)$ and a complex eigenvalue β. The special case with $\beta_i = 0$ gives neutral disturbances.

A MATLAB code[6] developed on the basis of a pseudo-spectral method, which eliminates spurious eigen values,[7] is used to solve the present eigenvalue problem. The code has been validated against the available literature results for the stability of a plane Poiseuille[8] and Hartmann[9] flows.

V. RESULTS AND DISCUSSIONS

The basic velocity profiles are obtained for different values of parameters Re, Gr and Ha using the analytical solution derived in Ref. 10 (Fig. 3). In all computations, the shape parameter *m* was set at *m*=1.0 that corresponds to the DEMO blanket conditions (see Table I). With this analytical solution the basic velocity profiles can be obtained for the values of *Re* and *Ha* corresponding to the blanket conditions but the solution has limitations in the maximum value of *Gr*, resulting in unrealistic velocity profiles if *Gr* >1e+08. Efforts are in progress to improve this analytical solution to reach higher values of *Gr*. The velocity profiles show strong internal shear layer at the center of the channel and a region of reverse flow near the "hot" wall at higher *Gr*.

The results of stability calculations using the numerical method described in Section IV are plotted in the form of a "neutral stability" curve obtained from the condition $\beta_i = 0$, which separates the stable and unstable solutions. The point on this curve where the Hartmann number is largest gives the critical Hartmann number. Above the critical Hartmann number all possible perturbation modes are damped, while below some modes are amplified.

Figure 4 shows neutral stability curves for two different sets of *Re* and *Gr*. Unlike the case of buoyancy assisted flows [2] presence of strong internal shear layer in buoyancy opposed flows increases their chance of becoming hydrodynamically unstable, the critical *Ha* for these flows increases by one order of magnitude compared to that of buoyancy assisted flows. As explained above, in the present study the maximum *Gr* is limited to 1e+08, however the results can be extrapolated to higher *Gr* to predict the flow regime under ITER and likely DEMO conditions. Under ITER conditions as shown in Table I, the *Gr* is one order of magnitude higher than the maximum one achieved in the present study. Simple extrapolation of the data in Fig. 4 to the ITER conditions gives the critical Hartmann number ~ 10^4, which is significantly higher than that in the ITER blanket. Therefore, the downward flows in the ITER blanket conditions are expected to be hydrodynamically unstable. Similar extrapolations could be done in the case of a DEMO blanket, resulting in the same conclusion. However, taking into account the big difference in *Gr* between the present study and the DEMO case (four orders of magnitude), this conclusion should be viewed as a preliminary one since a simple linear extrapolation may not be valid.

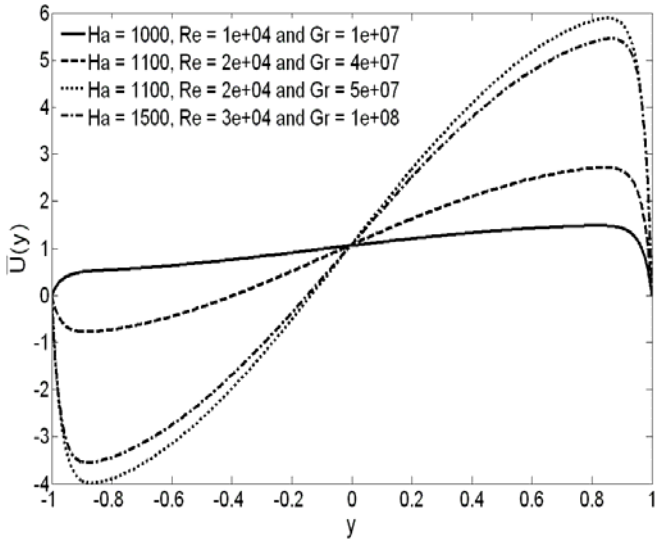

Fig. 3. Variation of basic velocity profile for different set of parameters *Ha*, *Re* and *Gr*.

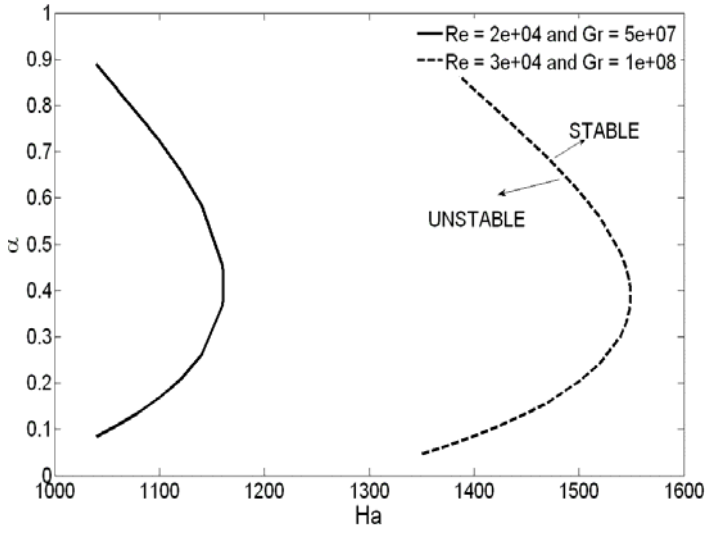

Fig . 4. Neutral stability curves for two different sets of *Re* and *Gr*.

Figure 5 shows the vorticity distribution for a particular set of parameters. The presence of a strong internal shear layer in the basic velocity profile results in a shear layer instability and a row of vortices appear at the center (primary instability), these vortices interact with the boundary layers near the walls and make them unstable resulting in a row of vortices near the walls (secondary instability).

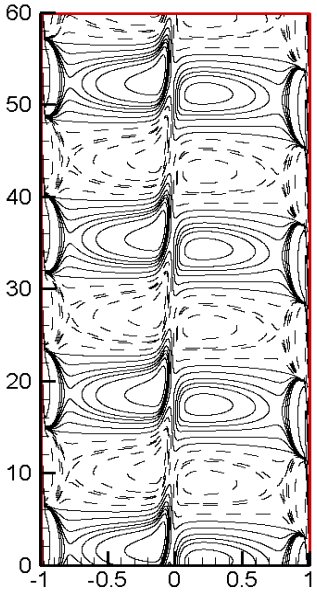

Fig. 5. Vorticity distribution showing a row of strong vortices at the center of the channel and near the walls for Ha = 1500, Re = 3e+04 and Gr = 1e+08.

VI. CONCLUSIONS

An approach developed to access conditions when the MHD mixed convection in long vertical ducts becomes unstable is used to perform linear stability analysis for the buoyancy opposed flows under the conditions relevant to the US DCLL blanket concept. The computations performed for two different set of parameters have revealed that these flows are prone to become hydrodynamically unstable with critical $Ha \sim 10^3$ which is comparable to the values that prevail under the blanket conditions. Two types of instability mechanisms were observed one corresponding to the strong internal shear layer in the basic velocity profile and the second corresponding to the boundary layer. As the stability analysis only predicts conditions when the flow becomes unstable there is a need to carry out full numerical calculations for these types of flows and to extend the analysis to higher values of the Grashoff number in the future to better understand the flow behavior and to address the effect of the pulsating flow on heat and mass transfer.

ACKNOWLEDGMENTS

The study has been performed under DOE grant DE-FG02-86ER52123-A040.

REFERENCES

1. S. SMOLENTSEV, R. MOREAU, M.ABDOU, "Characterization of Key Magnetohydrodynamic Phenomena in PbLi Flows for the US DCLL Blanket," *Fusion Eng. Des.,* **83**, 5 (2008).
2. N. VETCHA, S. SMOLENTSEV, M.ABDOU, "Theoretical study of mixed convection in poloidal flows of DCLL Blanket," *Fusion Sci. Tech.,* **56**, 2 (2009).
3. J. SOMMERIA, R. MOREAU, "Why, How and When MHD Turbulence Becomes Two Dimensional?" *J. Fluid Mech.,* **118**, 507 (1982).
4. S. SMOLENTSEV, N. MORELY, M. ABDOU, "MHD and Thermal Issues of the SiCf/SiC Flow Channels Insert," *Fusion Sci. Tech.,* **50**, 107 (2006).
5. YEN-CHO CHEN, J. N. CHUNG, "The Linear Stability of Mixed Convection in a Vertical Channel Flow," *J. Fluid Mech.,* **325**, 29 (1996).
6. J. A. C. WEIDEMAN, S. C. REDDY, "A MATLAB Differentiation Matrix Suite," *ACM Transactions on Mathematical Software,* **26**, 4, 465 (2000).
7. W. HUANG, D. M. SLOAN, "The Pseudospectral Method for Solving Differential Eigenvalue Problems," *J. Computational Physics,* **111**, 399 (1994).
8. S. A. ORSZAG, "Accurate Solution of the Orr-Sommerfeld Stability Equation," *J. Fluid Mech.,* **50**, 689 (1971).
9. R. C. LOCK, "The Stability of the Flow of Electrically Conducting Fluid Between Parallel Planes Under a Transverse Magnetic Field," *Proc. of the Royal Society of London, Series A, Mathematical and Physical Sciences,* **233**, 1192, 105 (1955).
10. S. SMOLENTSEV, R. MOREAU, M.ABDOU, "Study of MHD Mixed Convection in the DCLL Blanket Conditions," *7th PAMIR Conference on Fundamental and Applied MHD,* Giens, France, September 8-12, 2008.